

# Dynamical effects of electromagnetic flux on Chialvo neuron map: nodal and network behaviors

---

Sishu S. Muni, Hammed O. Fatoynbo, & **Indranil Ghosh**  
(@indraghosh314)

School of Mathematical and Computational Sciences  
Massey University, New Zealand



## Neurons as Dynamical Units

- Neurons represent important dynamical units of the brain.
- The dynamical behaviours of neurons, like firing of potentials for example, can be modeled as simple dynamical systems like ODEs or maps.

## Chialvo Map

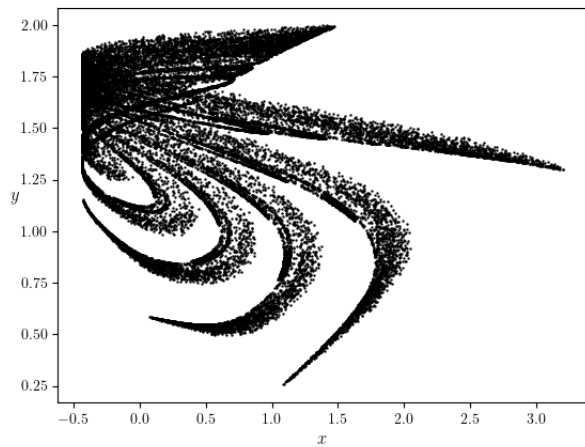
The two-dimensional discrete neuron system by Chilavo [D. R. Chialvo. **Generic excitable dynamics on a two-dimensional map. Chaos Solitons & Fractals, 5:461– 479, 1995.**] is given by the map

$$x_{n+1} = x_n^2 e^{(y_n - x_n)} + k_0,$$

$$y_{n+1} = ay_n - bx_n + c$$

- The state variables  $x$  and  $y$  represent the activation variable and recovery-like variable,
- $a, b, c$  and  $k_0$  are the system parameters,
- $a < 1$  is the time constant of recovery,
- $b < 1$  represents the activation dependence of the recovery process,
- $c$  denotes the offset, and
- $k_0$  is the time-independent additive perturbation.

## A Typical Phase Portrait



# Electromagnetic flux

We describe the effects of electromagnetic flux on the system of neurons with **memristors**. The induction current due to electromagnetic flux is given by

$$\frac{dq(\phi)}{dt} = \frac{dq(\phi)}{d\phi} \frac{d\phi}{dt} = M(\phi) \frac{d\phi}{dt} = kM(\phi)x.$$

- $\phi$ : electromagnetic flux across the neuron membranes,
- $k$ : electromagnetic flux coupling strength, &
- $M(\phi)$ : memconductance of electromagnetic flux controlled memristor.

We consider the following memconductance function:

$$M(\phi) = \alpha + 3\beta\phi^2.$$

## Improved Chialvo map under electromagnetic flux

Under the action of electromagnetic flux, the system of Chialvo map is improved to the following map:

$$x_{n+1} = x_n^2 e^{(y_n - x_n)} + k_0 + kx_n M(\phi_n),$$

$$y_{n+1} = \alpha y_n - \beta x_n + c,$$

$$\phi_{n+1} = k_1 x_n - k_2 \phi_n,$$

making the system a three-dimensional smooth map. The new variables  $\alpha, \beta, k_1, k_2$  represent the electromagnetic flux parameters.

# Fixed points of the improved system i

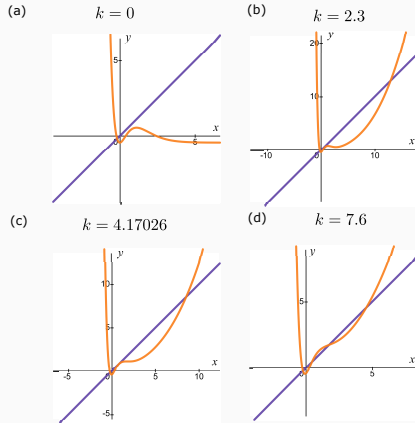
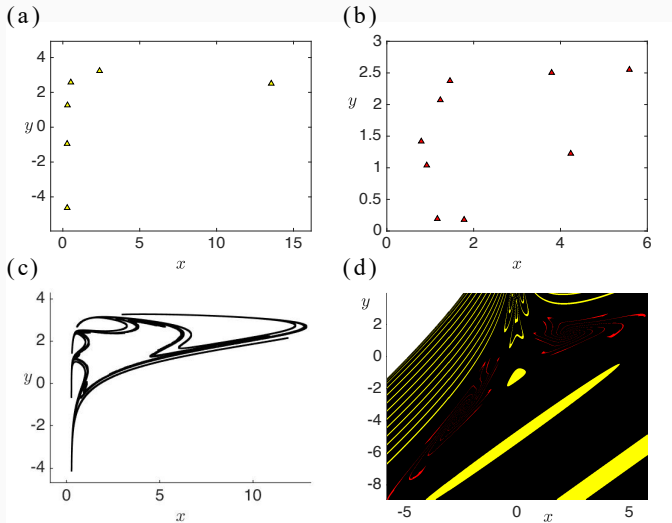


**Figure 1:** The parameters are set as  $a = 0.5$ ,  $b = 0.4$ ,  $c = 0.89$ ,  $k_0 = -0.44$ ,  $k_1 = 0.1$ ,  $k_2 = 0.2$ ,  $\alpha = 0.1$ ,  $\beta = 0.1$ .

# Multistability



# Bifurcation structures and antimonotonicity i

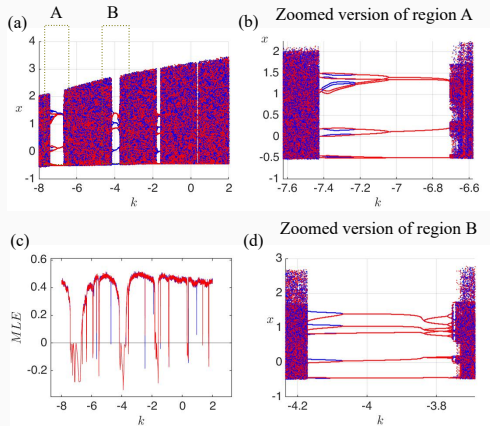


**Figure 2:** Bifurcation diagram of  $x$  with respect to  $k$  in panel (a). A maximal Lyapunov exponent diagram is shown in panel (b).

# Bifurcation structures and antimonotonicity ii

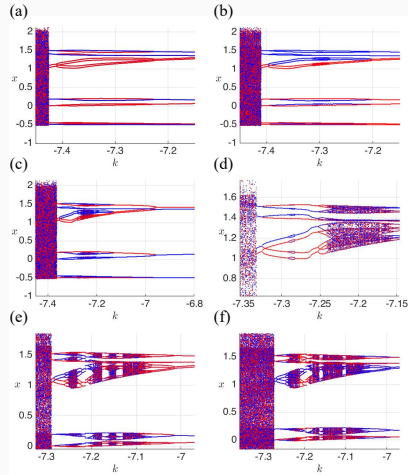


**Figure 3:** Bifurcation diagram of  $x$  with respect to  $k$  in panel (a). A maximal Lyapunov exponent diagram is shown in panel (c).

# Bifurcation structures and antimonotonicity iii

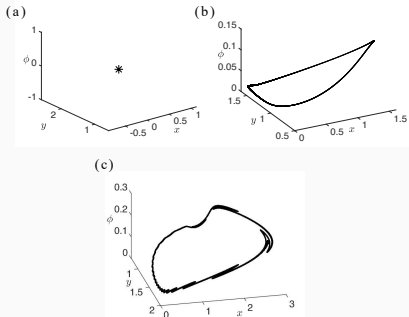


**Figure 4:** In (a) a stable fixed point is shown in the  $x - y - \phi$  phase space for  $a = 0.838$ . After a supercritical Neimark-Sacker bifurcation, an attracting closed invariant curve is born as shown in (b) at  $a = 0.841$ . A chaotic attractor is then formed when  $a$  is increased to 0.88.

# Evolution of fingered attractors

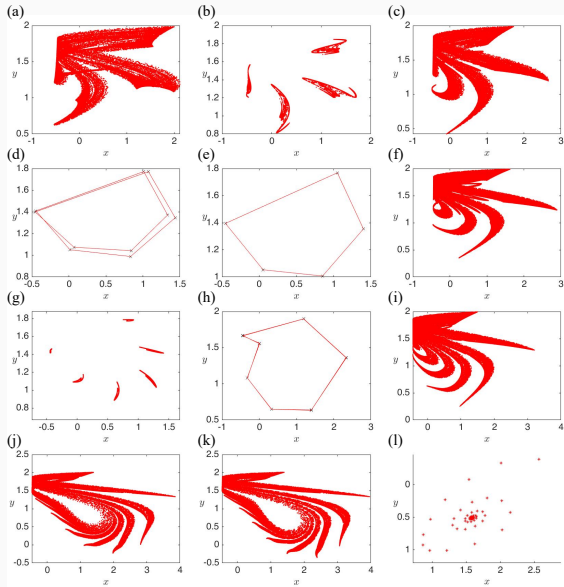
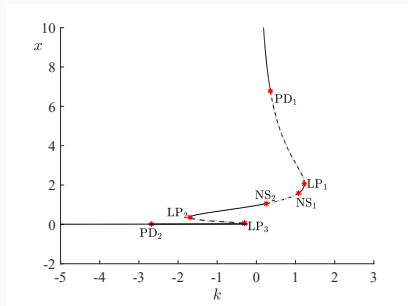


Figure 5: Evolution of fingered attractors with varying  $k$ .

# Numerical bifurcation analysis i

(a)



# Numerical bifurcation analysis ii

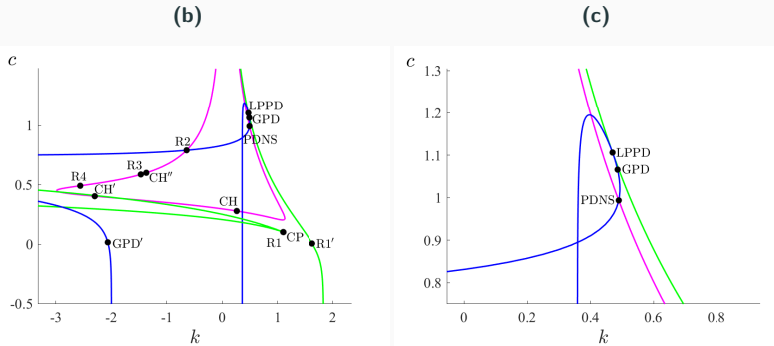


**Figure 6:** (a) Codimension-1 bifurcation diagram with  $k$  as bifurcation parameter. (b) Codimesion-2 bifurcation diagram in  $(k, c)$ -parameter plane.

# Numerical bifurcation analysis iii

**Table 1:** Abbreviations of codimension-1 and codimension-2 bifurcations

Codimension-1			
Saddle-node (fold) bifurcation	LP	Neimark-Sacker bifurcation	NS
Period-doubling (flip) bifurcation	PD		
Codimension-2			
Cusp	CP	Chenciner	CH
Generalized flip	GPD	Fold-Flip	LPPD
Flip-Neimark-Sacker	PDNS	Fold-Neimark-Sacker	LPNS
1:1 resonance	R1	1:2 resonance	R2
1:3 resonance	R3	1:4 resonance	R4

## Bursting and spiking features

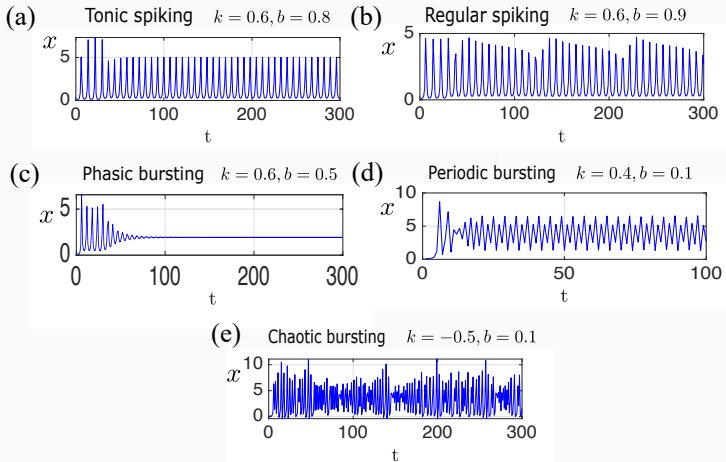


**Figure 7:** Various spiking and bursting patterns exhibited by the Chialvo neuron model under the action of electromagnetic flux.

## Ring-star network for multiple neurons i

The mathematical model for the ring-star connected Chialvo neuron map under electromagnetic flux is defined as:

$$\begin{aligned}x_m(n+1) &= x_m(n)^2 e^{y_m(n)-x_m(n)} + k_0 + kx_m(n)M(\phi_m(n)) \\&\quad + \mu(x_m(n) - x_1(n)) + \frac{\sigma}{2R} \sum_{i=m-R}^{m+R} (x_i(n) - x_m(n)),\end{aligned}$$

$$y_m(n+1) = ay_m(n) - bx_m(n) + c,$$

$$\phi_m(n+1) = k_1 x_m(n) - k_2 \phi_m(n),$$

## Ring-star network for multiple neurons ii

whose central node is further defined as

$$x_1(n+1) = x_1(n)^2 e^{(y_1(n)-x_1(n))} + k_0 + kx_1(n)M(\phi_1(n)) \\ + \mu \sum_{i=1}^N (x_i(n) - x_1(n)),$$

$$y_1(n+1) = ay_1(n) - bx_1(n) + c,$$

$$\phi_1(n+1) = k_1 x_1(n) - k_2 \phi_1(n),$$

having the following boundary conditions:

$$x_{m+N}(n) = x_m(n), \quad (1)$$

$$y_{m+N}(n) = y_m(n),$$

$$\phi_{m+N}(n) = \phi_m(n).$$

## Ring-star network for multiple neurons iii

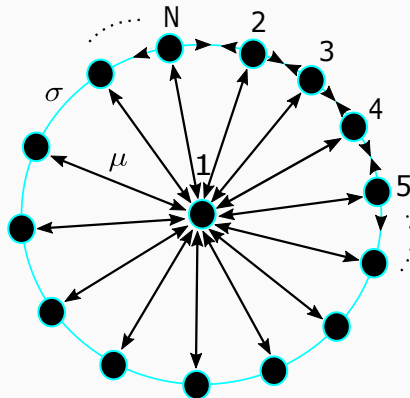


**Figure 8:** Ring-star network of Chialvo neuron system.

# Ring network

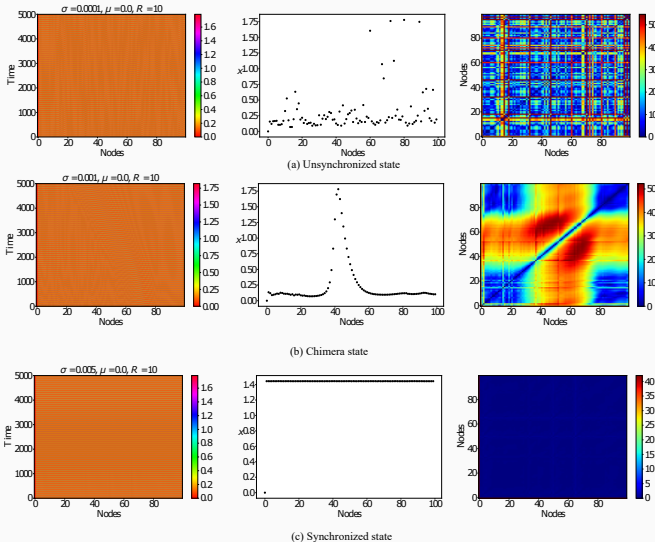


**Figure 9:** Ring network of Chialvo neuron ( $\mu = 0, \sigma > 0, k = 3.5$ ).

# Ring-star network

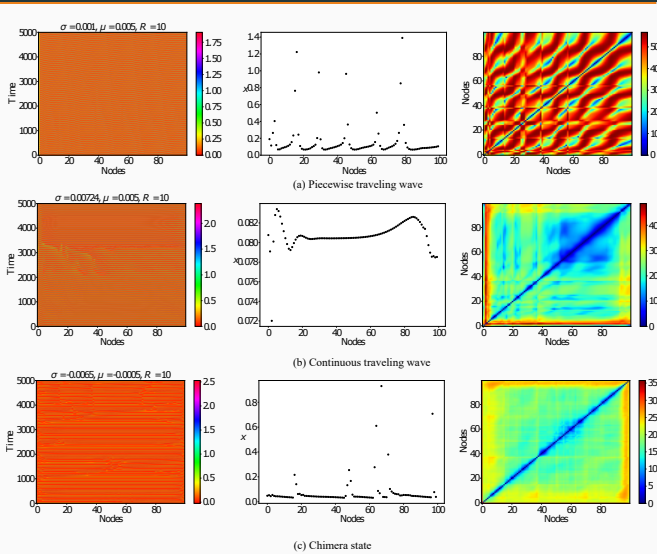


**Figure 10:** Ring-star network of Chialvo neuron.

## X-k plot

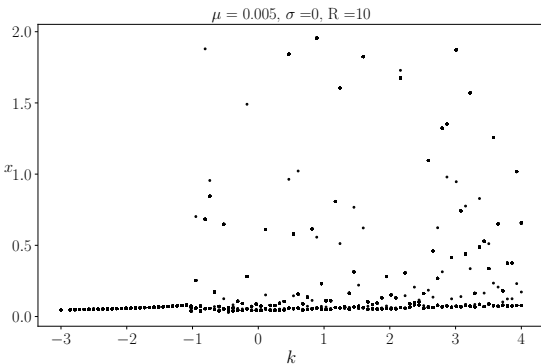


**Figure 11:**  $X - k$  plot for star network with  $\mu = 0.005$  and  $R = 10$ . This shows the intervals of  $k$  for the prevalence of single-cluster, multi-cluster states.

# Star network

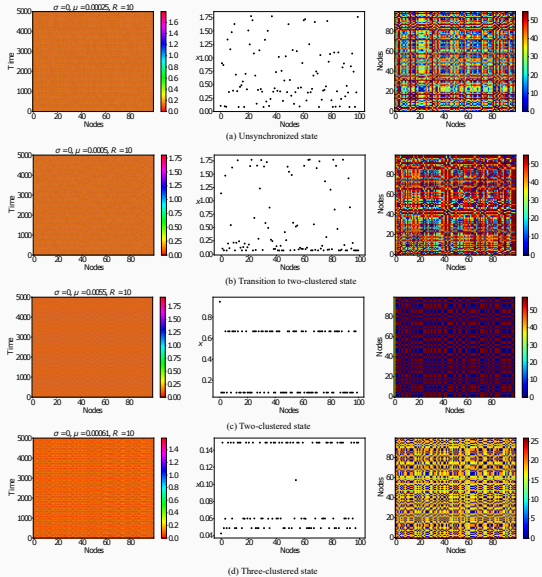
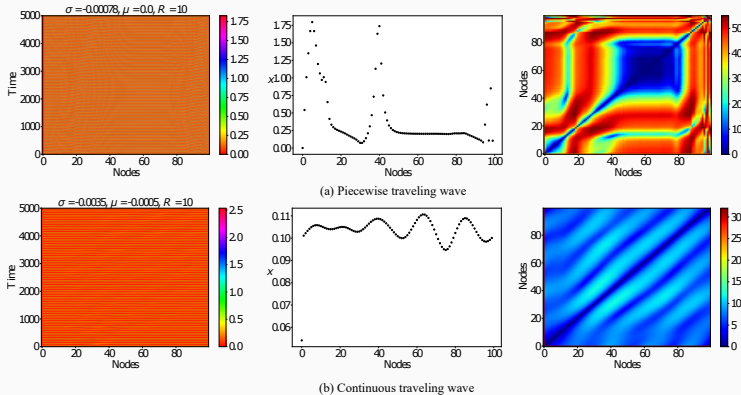


Figure 12: Star network of Chialvo neuron.

# Negative strength patterns



**Figure 13:** Negative-strength patterns of Chialvo neuron ( $\mu \leq 0, \sigma < 0$ ).

## Summary

1. We have studied the dynamical behaviours of discrete Chialvo neuron (single and network) under the application of an electromagnetic flux.
2. We have studied multistability, antimonotonicity, various routes to chaos, among other things for the system.
3. Traditional techniques adopted are bifurcation diagrams, Lyapunov exponent diagram, phase portraits, basins of attraction, and numerical continuation of bifurcations.
4. Scheduled to appear in the International Journal of Bifurcation and Chaos Vol. 32. Find our preprint at [arXiv:2201.03219](https://arxiv.org/abs/2201.03219).

**Thank you. Questions?**